The Value of Inflammatory Signals in Adaptive Immune Responses

Soumya Banerjee[1], Drew Levin[1], Melanie Moses[1], Frederick Koster[2], and Stephanie Forrest[1]

[1] Department of Computer Science, University of New Mexico, USA
[2] Department of Pathology, University of New Mexico, USA

Abstract. Cells of the immune system search among billions of healthy cells to find and neutralize a small number of infected cells before pathogens replicate to sufficient numbers to cause disease or death. The immune system uses information signals to accomplish this search quickly. Ordinary differential equations and spatially explicit agent-based models are used to quantify how capillary inflammation decreases the time it takes for cytotoxic T lymphocytes to find and kill infected cells. We find that the inflammation signal localized in a small region of infected tissue dramatically reduces search times, suggesting that these signals play an important role in the immune response, especially in larger animals.

1 Introduction

Rapid search is crucial for an effective immune response: Immune system cells must find, identify and neutralize pathogens before those pathogens replicate in sufficient numbers to cause disease or death. The adaptive immune system has a small number of pathogen-specific cells that must search for and neutralize a small number of initially localized pathogens in a very large tissue space. We investigate how inflammatory signals accelerate this search.

The adaptive immune response must conduct two "searches" to neutralize pathogens. First, recirculating antigen-specific T and B cell precursors must interact with antigen-loaded dendritic cells, and the architecture of the lymph node facilitates this interaction [1–3]. The second search is T cells activated in the lymph node efficiently finding and neutralizing infected cells in tissue with the help of inflammatory signals. In this paper we analyze these two searches in response to influenza infection in the lung.

CTLs are activated within the infected site LN and are released into the bloodstream where they travel through a branching network of arteries until they reach a capillary in the lung. Capillaries in infected regions of the lung are permeated by an inflammatory signal which causes CTLs to exit the capillary and enter the lung tissue, where a chemokine gradient guides the CTL to infected cells. When CTLs recognize the antigen displayed on the surface of infected cells, they neutralize those cells. The information represented by the inflammatory signals is local, and occurs in an initially small region of the lung

surface, possibly as small as a few mm^2 in a 100 m^2 surface area in a human lung [17]. We ask how much the local inflammatory signal reduces the time for CTLs to find the site of infection and eradicate the influenza pathogen. Without an inflammation signal indicating which capillaries are near infected tissue, CTLs would have to exit capillaries in random locations and begin a slow random walk (at speeds measured in microns per minute) through the large area of lung tissue to search for the site of infection. With the inflammatory signal, CTLs can exit the relatively fast flow of the circulatory network only when they are in close proximity to infected cells.

In this paper we describe two sets of models. The first (null) model predicts how long it would take for CTLs to find infected cells by searching via a random walk through the entire lung tissue. The second set of models are simplified representations of how inflammatory signals guide CTL search in real immune systems. This second set of models is parametrized from experimental data. By comparing predictions of the null model to the more realistic model with inflammation, we estimate how much the inflammatory signal reduces the time for CTLs to find and eradicate influenza.

We use ordinary differential equation (ODE) and agent-based models (ABM) to quantify the value of the inflammatory signal, measured as the decrease in the time it takes for CTLs to both find and eradicate virus from the lung. The ABM incorporates the spatial aspect of virus spread and CTL mediated killing of infected cells, and the ODE model can scale up to realistic cell population sizes. In both cases, we first model an immune response without inflammatory signals where CTLs exit to tissue at the first capillary they encounter and search by random walks until they find a chemokine gradient that guides them to the infected cells. Second, we model an immune response with inflammatory signals where CTLs exit to tissue only when the capillary has an inflammatory signal. If there is no signal, CTLs recirculate through the cardiovascular network until they find an inflamed capillary. We suggest that localized signals like the inflammatory signal are enormously important to immune function. Here we take a first step toward quantifying the value of that signal in terms of time required to get T cells to sites of infection and to control influenza infection. This has important consequences for understanding the role of information signals in immune systems more generally, and also the role that local information signals can play in other complex biological systems [11, 12] and in artificial immune systems where decentralized search requires effective use of local signals to solve computational problems [2, 3].

The remainder of the paper reviews relevant features of the immune system (Section 2), outlines our hypotheses (Section 2), and describes the models (Sections 4 and 5). Section 4 presents the ODE model and compares its predictions to empirical data. Section 5 uses the ABM to verify some of the ODE predictions and produce more realisitic spatially explicit simulations, including pathogen spread during the CTL search. We conclude by quantifying how much inflammatory signals improve immune response in these models.

2 A Review of the Relevant Immunology

This study characterizes how a key type of adaptive immune cells (cytotoxic T lymphocytes, also called $CD8^+$ T cells or CTLs) [6] search for and neutralize a common respiratory tract pathogen (influenza) in the principal target organ, the lung (Fig. 1). Among the many immune cells and molecules involved in providing defense against influenza [14], there is a complex set of interactions to guide CTLs to the site of infection and to produce chemokines and other information signals to help contain the infection. We simplify the array of chemokines with a single signal that causes inflammation and attracts CTLs to site of infection.

Infection begins when influenza virus is inhaled into the lung. It enters epithelial cells lining the airways and the air sacs (alveoli) of the lung. Epithelial cells initiate the first line of innate immune defense through the activation of interferon and the secretion of chemokines to attract inflammatory cells such as macrophages [10]. Inflammation increases local blood flow to the infected region and amplifies the chemokine signal. To initiate the adaptive immune response, resident lung dendritic cells capture virus and carry it to the draining lymph nodes (LN). LNs provide a dense tissue in which T and B lymphocytes and antigen-loaded dendritic cells encounter each other efficiently. Antigen-specific CTLs are activated within the LN, undergo cell division, and leave the LN to enter the blood circulation. We focus on the response of cytotoxic T lymphocytes (CTLs) because recovery from influenza pneumonia in wildtype mice has been shown to require neutralization of infected cells by CTLs [8].

The cardiovascular network in the lung follows the fractal branching of the airways.The branching arterioles end in a capillary network which nourishes the airsacs (alveoli) of the lung. The capillary density in mouse lung is approximately $5000/cm^2$ (estimated from [17]). The surface area of a mouse lung is approximately $100cm^2$ giving 500,000 capillaries in the mouse lung. Capillary density decreases as $M^{-1/4}$ where M is organism body mass [18, 17] and since humans are 10,000 times larger than mice, the capillary density in a human lung is $500/cm^2$. The surface area of a human lung is approximately $100m^2$ and hence the number of capillaries in a human lung is approximately $5 \cdot 10^8$.

The CTL flow through the arterial network without any signal to guide them to the tiny fraction of capillaries near the initial infection. If an activated CTL reaches an inflamed capillary, it exits the capillary into lung interstitial tissue. The tissue surrounding inflamed capillaries also contains a chemokine gradient which the CTL follows to locate infected epithelial cells and reduce viral replication. The chemotactic signals are composed of cytokines and chemokines which provide a region of attraction larger than that provided by antigen and infected cells. If an activated CTL reaches an uninflamed capillary, it may wander short distances through the capillary network. If it still does not encounter an inflammatory signal, it recirculates through the blood and eventually returns to another capillary in the lung. The recirculation time for mice is 6 seconds and 60 seconds for humans [13].

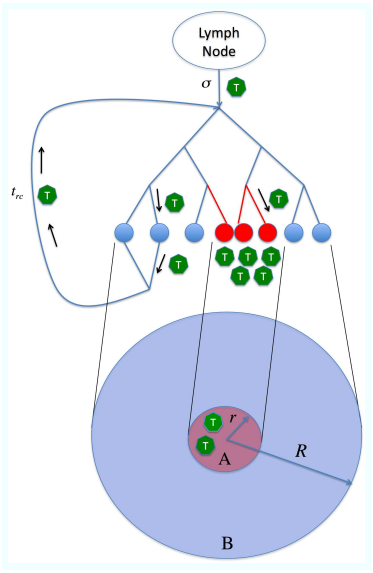

Fig. 1. A region (A of radius r) of infected tissue, chemokines and inflammatory signals, surrounded by region B which does not have any infected cells, inflammation or chemokines. CTLs (green hexagons) leave the LN at rate σ and travel through the branching arteries to capillaries. If capillaries are inflamed (in region A) CTLs exit capillaries and search for infected cells (small red circles) in lung tissue. If the capillaries are not inflamed (in region B) the CTLs recirculate.

3 Goals and Hypotheses

Inflammatory signals and chemotactic gradients are examples of signals that serve to guide search processes in the adaptive immune system. We hypothesize that these and other signals enable the activated immune cells to find and neutralize pathogens more quickly than in the absence of such signals. More specifically, we aim to quantify the benefit provided by the inflammation in the capillaries, which allows circulating CTLs to know that they have reached a site of infection.

We examine a hypothetical immune response without inflammatory signals (CTLs searching for infected tissue by randomly walking through lung tissue) and a more realistic immune response with inflammatory signals (CTLs recirculate through the arterial network until the presence of inflammation signals them to exit near infected tissue). We study how long it takes for the first CTL to find the infected region, how quickly CTLs accumulate in infected tissue, and how many epithelial cells become infected in a specified time period. We quantify the value of the information signal as the ratio of these values with inflammatory signal to those values without the signal. We use ODE and ABM to estimate the value of the inflammation signal. The ODE can model large numbers of

cells, so we use ODEs to compare the value of the inflammatory signal in mice and humans. We then use an agent based model to investigate the dynamics of infection growth and spatial interactions between cells in the mouse.

4 Ordinary Differential Equation Model

In this section we analyze how quickly CTLs arrive at the site of infection with and without an inflamation signal using an ODE model. We represent the region of infection as a circular area (region A) of radius r of tissue expressing a general chemotactic signal. This region is surrounded by a region of uninfected tissue (a concentric circle of radius R (region B)) without inflammation or chemokines.

Any activated CTLs that flow to capillaries in region A will have an inflammatory signal that causes the CTL to exit the capillary and a chemokine gradient that will direct those CTLs to infected cells. In contrast, CTLs that arrive in the lung via capillaries in region B will have no inflammatory signal and no chemokines to guide them to the infected cells in region A. We assume that CTLs that exit into tissue do not go back into circulation.

There are several simplifying assumptions in the ODE model. It ignores viral replication and assumes that the infected region A is a fixed size. It also ignores the movement of CTLs inside capillaries, and instead assumes that CTLs either immediately sense inflammation and exit into tissue or immediately recirculate. The model also ignores CTL death in the lung.

The dynamics of the system are represented by coupled ODEs. We parameterize the ODEs to consider two cases. In the first case, CTLs search for virus using only the random walk (null model). In the second case, CTLs in region A receive an inflammation signal that allows them to exit and follow the chemotactic gradient, while CTLs in region B continue to recirculate through the lymph system until they find an inflamed capillary in region A as in Fig. 1.

4.1 ODE Model 1: CTL Search Without an Inflammation Signal

In this scenario there is no signal to direct CTLs to an infected region, therefore CTLs always exit into tissue as soon as they reach a capillary. The capillaries are assumed to be uniformly distributed througout the lung, and a single activated lymph node is assumed to produce activated CTLS at a fixed rate of σ CTLs per hour. The infection is in a region of constant radius r, and the lung surface is a circle of radius R. The time taken for CTLs to circulate through the lymph system is denoted by t_{rc}. The combined system is represented by the following differential equations:

$$\frac{dN_c}{dt} = \sigma - \frac{N_c}{t_{rc}} \tag{1}$$

$$\frac{dN_w}{dt} = \frac{(R^2 - r^2) \cdot N_c}{R^2 \cdot t_{rc}} - \frac{D \cdot N_w}{\pi((2/3(R-r)+r)^2 - r^2)} \tag{2}$$

$$\frac{dN_f}{dt} = \frac{r^2 \cdot N_c}{R^2 \cdot t_{rc}} + \frac{D \cdot N_w}{\pi((2/3(R-r)+r)^2 - r^2)} \tag{3}$$

Equation (1) describes the change in the number of recirculating activated CTLs in the cardiovascular system (N_c) due to the rate of production of new CTLs in the LN (σ) and time it takes CTLs to travel to the capilaries (t_{rc}). Since the relevant time step in this setting is the minimum time taken for CTLs to complete one circuit through the arterial and venous circulation system (the recirculation time t_{rc}) and is different from the simulation time step (dt), all rate constants are divided by t_{rc}.

Equation (2) describes the change in the number of CTLs (N_w) that are doing a random walk in tissue and searching for infected cells. The change in N_w is due to the rate at which CTLs exit into region B from circulation (a fraction of $\frac{N_c}{t_{rc}}$) and the rate at which these searching CTLs find region A. The fraction of circulating CTLs that enter capillaries in region B is given by the relative area of region B ($\frac{R^2-r^2}{R^2}$). The rate at which CTLs find region A is calculated as follows: an average CTL in region B will be at a distance 2/3 from the periphery of region A (obtained by integrating over all CTLs at each distance in region B). The mean area that this CTL will cover before reaching region A is given by the quantity $\pi((2/3(R-r)+r)^2 - r^2)$, and the mean time in which this area is covered is this quantity divided by the diffusion constant for random walk (D), again adjusted for the recirculation time. The reciprocal of this time gives the rate at which a single CTL enters region A. To complete the analysis we multiply this quantity by the number of searching CTLs. Finally, Equation (3) describes the change in the number of CTLs (N_f) that have found infected cells (in region A). This is composed of the searching CTLs from Equation (2) that find the infected region and the fraction of the recirculating CTLs from Equation (1) that enter capillaries in region A (represented by the area of region A relative to the total lung area). We use the model to study the arrival of CTLs at the site of infection, first in the mouse lung and then in the human lung.

In order to numerically integrate Equations (1)-(3) we first estimate the diffusion rate of CTLs. Since we are not aware of any published values for diffusion rates of activated CTLs within tissue, we used measured mean square displacements of T cells within the LN [4]. Following Beauchemin et al. [4], the equation relating mean square displacement of a random walking particle in two dimensions at time t is given by $\mid m \mid = \sqrt{4Dt}\frac{\Gamma(\frac{3}{2})}{\Gamma(\frac{1}{2})}$ where $\mid m \mid$ is the mean square displacement, D is the diffusion constant and Γ is the gamma function. We estimated D as $56(\mu m)^2/h$ in the LN [4], and we use this value to characterize the random walk in lung tissue.

We estimate the parameter σ from experimental data (detailed in the next section) as 864 activated CTLs per hour, and the time to recirculate (t_{rc}) is 6 seconds [5]. The area of infection has a radius (r) of 1 mm (personal observation for seasonal strains in mice) and the total lung surface is represented by a circle with a radius of 10 cm (R) [17].

The model shows that there is a steady state of approximately 2 circulating activated CTL. So few CTLs are in circulation because they exit the LN approximately 1 every 4 seconds and spend only 6 seconds in blood before immediately exiting the blood to search in the lung. We numerically simulated the ODE system and found that the time for the first CTL to reach the site of infection (region A) is approximately 12 hours post activation in the LN (Fig. 2, Panel A). Approximately 10 CTLs find the infected region at day 5 post activation.

Next we use ODE Model 1 to predict how quickly CTLs arrive at the infected site in a human. Human body mass is approximately 10,000 times larger than a mouse. Human lungs are a corresponding 10,000 times greater area, so R becomes 10 meters [17]. We assume that the initial area of infection r remains the same 1mm^2. CTL recirculation time (t_{rc}) increases to 60 seconds [5].

In order to calculate the rate of CTL production from LN (σ) we scale the (σ) estimated for mice by a factor of $M^{3/7}$ following [3]. This scaling assumes that LNs in larger animals are larger and have more high endothelial venules to release activated CTLs at a faster rate. From this we estimate σ as approximately 45000 CTLs per hour. Numerically simulating the ODE system, we predict the time for a CTL to find an infected cell in a human lung as approximately 90 days, which is much longer than the actual time taken to resolve influenza infections (approximately 10 days) [8].

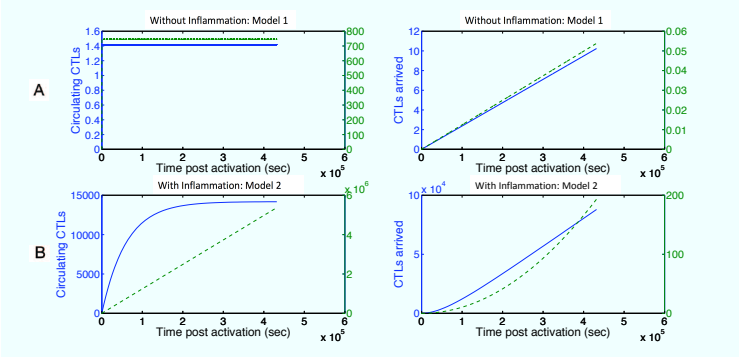

Fig. 2. Row A: The number of circulating CTLs (N_c) and CTLs that have arrived at the site of infection(N_f) vs. time post activation of the first CTL in LN for CTLs searching without an inflammatory signal (ODE Model 1) for mice (blue, left axis) and humans (green dotted, right axis). The number of recirculating CTLs reaches a steady state because once they enter the lung they never recirculate. Row B: N_c and N_f vs. time post activation for CTLs circulating in the presence of inflammatory signals (ODE Model 2 fit to experimental data) for mice (blue, left axis) and humans (green dotted, right axis). Note the difference in y-axis scale between the two rows.

4.2 ODE Model 2: CTL search with an Inflammatory Signal

Here we model an immune response with inflammatory signals. CTLs exit capillaries and enter lung tissue only when there is an inflammatory signal in the capillary. All other parameters are identical to ODE Model 1. The system is represented by the following differential equations:

$$\frac{dN_c}{dt} = \sigma - \frac{r^2 \cdot N_c}{R^2 \cdot t_{rc}} \tag{4}$$

$$\frac{dN_f}{dt} = \frac{r^2 \cdot N_c}{R^2 \cdot t_{rc}} \tag{5}$$

Equation (4) describes the change in the number of circulating activated CTLs circulating in the cardiovascular system (N_c). (N_c) changes due to the addition of new CTLs from the LN at rate (σ), and the loss of CTLs from circulation that exit capillaries expressing inflammatory signals and enter infected tissue (region A). Equation (5) describes the increase in the number of CTLs that find infected cells. This is the same as the loss term from the pool of recirculating CTLs from Equation (4).

We fit Model 2 to experimental numbers of CTLs in lung at various time points post infection for influenza in mice [8]. The fitting procedure found free parameters that minimized the mean squared error between the model and the data. We only considered data up to the peak of CTL activation and did not consider the decline of CTLs after the infection is cleared.

Model 2 (Equations 4 and 5) was solved numerically using Berkeley Madonna [7]. The curve fitter option in Berkeley Madonna (Runge-Kutta 4, step size = 0.0004 sec) was used to establish the best-fit parameter estimates. The curve-fitting method uses nonlinear least-squares regression that minimizes the sum of the squared residuals between the experimental and predicted values of N_f.

Next we compared model output for mice and humans. For mice, we fixed r to 1 mm, R to 10 cm, and the recirculation time (t_{rc}) to 6 seconds. We then estimated the LN rate of output of CTLs (σ). The best fit estimate for σ was approximately 864 activated CTLs per hour. Model output is shown in Fig. 2 Panel B (a list of all ODE model parameters is given in Table 1). Numerically simulating the ODE system, we estimated the time taken for the first CTL to reach infected tissue to be approximately 15 minutes (Fig. 2 Panel B). Approximately 80000 CTLs find the infected region at day 5 post activation. We modeled CTL search in the human lung using the same values as in ODE Model 1 ($R = 10$ meters, $t_{rc} = 60$ seconds and $\sigma = 45000$ CTLs per hour) and numerically simulated the ODE system. The predicted time for an activated CTL to discover an infected cell in a human lung is approximately 8 hours, and the number of CTLs that reach the lung by 5 days post activation in the LN is approximately 190.

In summary, the presence of an inflammatory signal and a chemokine gradient around infected cells results in a earlier first discovery of infection by activated CTLs in both mice and humans. In mice, the first CTL with inflammation arrives in 15 minutes compared to 12 hours without it, a 48-fold speedup. The

inflammation signal reduces search time in humans more than in mice: The first CTL with inflammation arrives in 8 hours compared to 90 days without it, a nearly 270-fold speedup.

Table 1. The parameters used in the ODE and ABM for mice with a short description of their role and default value ([§] measured in human cell lines)

Description	Value	Source
Release rate of activated CTLs (σ)	$864/h$	Fit to data in [8]
CTL recirculation time (t_{rc})	$6\ s$	[13]
CTL diffusion coefficient (D)	$56(\mu m)^2/h$	Calculated from [4]
Radius of lung area (R)	$10cm$	[17]
Radius of circle lung infected area (r)	$0.1cm$	Personal observation
Length of cubic ABM simulation compartment	$2000\mu m$	Model parameter
Time between infection and secretion [§]	$10.5h$	[9]
Duration of productive infection [§]	$17.15h$	[9]
ABM virus secretion rate [§]	$2.6\ virions/h$	[9]
ABM CTL sensing radius	$10\mu m$	Model parameter
ABM Epithelial cell diameter	$10\mu m$	Model parameter
ABM CTL diameter	$4\mu m$	Model parameter

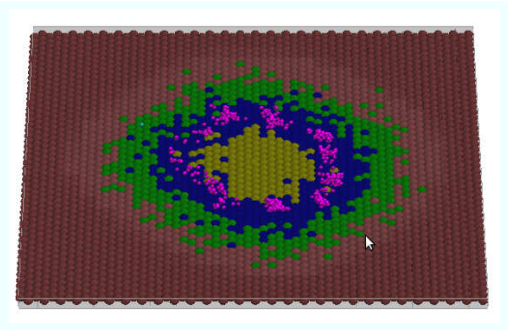

Fig. 3. A snapshot of the CyCells ABM in action. The epithelial cell layer is made up of healthy cells (dark red), infected incubating cells (green), virus expressing cells (blue), and dead cells (yellow). The area of lighter red surrounding the infection shows that free virus particles (semi-transparent white) are present. T-cells (pink) are seen swarming over locations with high virus concentration.

5 Agent Based Model

The ABM extends the earlier results to consider spatial and stochastic effects of CTL migration and recirculation, also incorporating infection spread and CTL mediated killing of infected cells. The CyCells [16, 15] modeling tool explicitly represents healthy cells, infected cells, and CTLs, and represents cytokines, chemokines, and virus as concentrations. We model the release of virions from infected cells, diffusion of chemokines and inflamatory signals, and chemotaxis of CTLs up a chemokine gradient. A screenshot of the graphical representation is shown in Fig. 3.

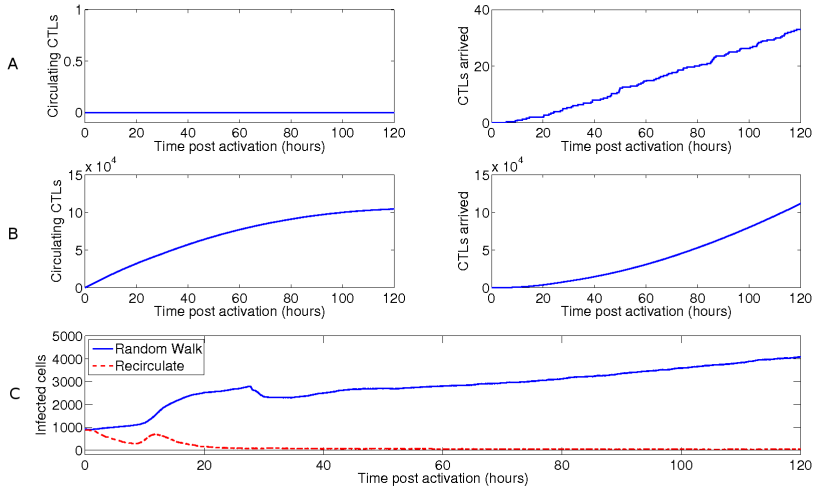

Fig. 4. Panel A: Plot of the number of recirculating CTLs (N_c) and CTLs that have found infected cells (N_f) vs. time post activation for CTLs only walking randomly (ABM 1). Panel B: Plot of N_c and N_f vs. time for CTLs only recirculating (ABM 2). Panel C: Plot of the number of infected cells over time for ABM 1 and ABM 2. The population bumps in Panel C during the first day post activation are an artifact of the model initialization scheme and do not affect the final results.

5.1 ABM Model 1: Dynamics without Inflammation

We start by modelling a $2mm$ by $2mm$ grid with an area of infection that represents five days of growth in the absence of a secondary immune response. After five days, specific CTLs become activated and enter the grid at a random location at $\sigma = 864/hour$, scaled down to adjust for the $4mm^2$ subset of the $10cm \times 10cm$ area of the mouse lung. In ABM Model 1, there is no inflammatory

signal, so CTLs that enter the grid immediately exit the capillary and begin a random walk through lung tissue. Infected cells produce virions which then infect healthy cells. Virus infected cells are differentiated into two populations: infected cells that are incubating but not secreting virus, and expressing cells that are actively producing new virions. The parameters describing rate of infection of healthy cells are taken from a previous study [9] (summarized in Table 1). Our primary results comparing system dynamics with and without inflammation signals do not depend on these parameters.

The time taken for the first CTL to detect an infected cell is 90 minutes. 33 CTLs find the infection five days post activation (Fig. 4 Panel A). There are 4,077 infected cells five days post activation.

5.2 ABM Model 2: Dynamics with Inflammation and CTL Recirculation

Next we study an immune response with inflammatory signals. We simulated an influenza infection using the same parameters as ABM 1, but allowed CTLs to recirculate until they encountered an inflammation signal. We evaluate the value of the inflammatory signal by comparing the results of ABM 1 and ABM 2.

The time taken for the first CTL to find an infected cell is 3.3 minutes. The number of CTLs which find infected cells in 5 days is 111,572 compared to 33 in ABM 1 (Fig. 4 Panel C). The number of infected cells remaining in the simulation is much lower for ABM 2 (46.7) compared to ABM 1 (4,077). Hence the value of the inflammation signal is a reduction in the number of infected cells at day 5 (from approximately 4,077 without an inflammatory signal to approximately 47 with the signal).

Table 2. The effect of inflammation on the time taken by CTLs to first detect infection, the number of CTLs that arrive in the infected region by day 5 post activation and the number of infected cells in the simulated lung tissue by day 5 post activation. ABM means and standard deviations are from three independent runs of each ABM.

Mice		Without Inflammation	With Inflammation	Benefit of Inflammation
Time to first detection	**ODE**	12 hr	15 min	**48**
	ABM	90 min ± 31.3 min	3.3 min ± 1.9 min	**27**
Arrived CTLs	**ODE**	10	80,000	**8,000**
	ABM	33 ± 4.6	111,572 ± 1,536	**3,380**
Infected cells	**ODE**	-	-	-
	ABM	4,077 ± 518	46.7 ± 4.7	**87**

Humans		Without Inflammation	With Inflammation	Benefit of Inflammation
Time to first detection	**ODE**	90 days	8 hr	**270**
Arrived CTLs §	**ODE**	0.05	190	**3,800**
Infected Cells §	**ODE**	-	-	-

6 Discussion

6.1 Summary of Results

In this study we used ODE and ABM models to quantify how much inflammation of infected tissue improves the adaptive immune response. This is measured in terms of three different values: how much the inflammatory signal speeds up the arrival of the first CTL at the site of infection; how much the inflammatory signal increases the number of CTLs that find the site of infection five days after CTL activation; and how much the inflammatory signal decreases the number of infected cells at five days after CTL activation. We used ODE and ABM models to quantify these improvements in mice and the results are summarized in Table 2. The speed up for the first CTL to arrive in the infected region in a mouse is tens of times faster in both the ODE and ABM models. The number of CTLs that reach the infected region by day five post activation is thousands of times faster in both models. The ABM includes CTL mediated killing of infected cells and predicts that with an inflammatory signal, the number of infected cells at day five is 87 times lower.

We scaled up the ODE model to make the same predictions for the human lung which is 10,000 times larger than the mouse lung. The ODE models predict that with an inflammatory signal the speed up in arrival of the first CTL humans is 270 times faster and 3800 times more CTL arrive at the site of infection at day five. Thus, the inflammatory signal improves the CTL search much more in the human than in the mouse.

6.2 Caveats and Limitations

We have made many simplifying assumptions in our models. We have ignored death of activated CTLs. We have assumed that LNs produce activated CTLs at a constant rate. We have ignored the time that activated CTLs spend in transit through a capillary network before going back into circulation if there is no inflammation. Because our interest is in the effect of a single signal (the inflammation signal the causes CTL to exit circulation and enter lung tissue near the site of infection), we ignore a vast array of signaling mechanisms and complex interactions between innate and adaptive immune system cells.

However, our assumptions and simplifications do not affect our primary conclusions about the relative speed of CTL search with and without an inflammatory signal. For example including a death rate of activated CTLs would give us a slightly higher estimate of the rate at which LNs release activated CTLs (σ) which would decrease search times with and without an inflammatory signal. Incorporation of a time dependent rate (σ) would give us more accurate production rates, but, again, this would change search times with and without an inflammatory signal in similar ways. Our conclusions that inflammation greatly speeds up CTL search in the lung depends primarily on two assumptions: first the relative speed of the random walk of CTL in the lung vs the speed of circulation, and second, the initial size of the infected region and its rate of growth.

6.3 Conclusions

Together, the ODE and ABM allow us to quantify the value of an information signal in biologically relevant terms. The local inflammation signal in the capillary allows search to be faster because it allows CTLs to recirculate when they arrive in capillaries in uninflamed regions of the lung. Because the lung surface area is so large, and CTL that have exited capillaries move so slowly relative to circulating CTL, this information signal drastically changes the ability of CTL to search the lung quickly. It allows CTL to effectively search the large surface area of the lung in the relatively fast flow of the blood circulatory system, and to exit only very near the site of infection. Further, because the human lung is 10,000 times larger than the mouse lung, the search for an initially small site of infection is much more difficult. This work shows that the effect of the local inflammatory signal is much larger in the search for influenza in the human lung vs the mouse lung. This suggests that the role of inflammation, chemokines and other immune signals may be different in humans and mice. Understanding these differences is important because so much knowledge of immunology and vaccine design depends on experimental work in mouse models.

The implications of this work extend beyond CTL search for influenza in the lung. An effective immune response often requires finding rare localized sites of infection. Models can make important contributions to our understanding of immune function by explaining how the multitude of immune signaling mechanisms improve such search processes.

By understanding the role of information signals in the immune system we can build models that allow us to understand how immune systems form distributed information exchange networks to search, adapt and respond to infections. Without central control, the interactions among millions of communicating components enable immune systems to search and respond to complex, dynamic landscapes effectively. We hypothesize that ant colonies, immune systems and other complex biological systems use common informational strategies to allocate components effectively to tasks and direct their search in space [11].

Our approach may be useful for developing decentralized search in Artificial Immune Systems [2, 3]. We anticipate that a quantitative characterization of information flow and its effect on performance will help us understand why systems of different sizes and in different environments use different information, organizational structures and strategies to accomplish similar tasks.

7 Acknowledgements

We thank Neal Holtschulte for suggesting the use of ODEs to model recirculation. This work is supported by grants from the National Institute of Health (NIH RR018754), DARPA (P-1070-113237) and National Science Foundation (NSF EF 1038682).

References

1. Banerjee, S., Moses, M.: A Hybrid Agent Based and Differential Equation Model of Body Size Effects on Pathogen Replication and Immune System Response. In: P.S. Andrews et al. (Eds.) Artificial Immune Systems, 8th International Conference, ICARIS 2009, Lecture Notes in Computer Science. vol. 5666, pp. 14–18 (2009)
2. Banerjee, S., Moses, M.: Modular RADAR: An Immune System Inspired Search and Response Strategy for Distributed Systems. In: E. Hart et al. (Eds.) Artificial Immune Systems, 9th International Conference, ICARIS 2010, Lecture Notes in Computer Science. vol. 6209, pp. 116–129 (2010)
3. Banerjee, S., Moses, M.: Scale Invariance of Immune System Response Rates and Times: Perspectives on Immune System Architecture and Implications for Artificial Immune Systems. Swarm Intelligence 4(4), 301–318 (2010)
4. Beauchemin, C., Dixit, N., Perelson, A.: Characterizing T Cell Movement within Lymph Nodes in the Absence of Antigen. The Journal of Immunology 178, 5505–5512 (2007)
5. Calder, W.: Size, Function and Life History. Dover Publications (1984)
6. La Gruta, N., Doherty, P.: Influenza Virology Current Topics, chap. Quantitative and qualitative characterization of the CD8+ T cell response to influenza virus infection. Caister Academic Press (2006)
7. Macey, R.I., Oster, G.: Berkeley Madonna, version 8.0. Tech. rep., University of California, Berkeley, California (2001)
8. Miao, H., Hollenbaugh, J., Zand, M., Holden, W., Mosmann, T., Perelson, A., Wu, H., Topham, D.: Quantifying the Early Immune Response and Adaptive Immune Response Kinetics in Mice Infected with Influenza A Virus. Journal of Virology 84(13), 6687–6698 (2010)
9. Mitchell, H., et al.: Higher replication efficiency of 2009 (h1n1) pandemic influenza than seasonal and avian strains: kinetics from epithelial cell culture and computational modeling. Journal of Virology pp. JVI.01722–10 (2010)
10. Moser, B., Loetscher, P.: Lymphocyte Traffic Control by Chemokines. Nature Immunology 2, 123–128 (2001)
11. Moses, M., Banerjee, S.: Biologically Inspired Design Principles for Scalable, Robust, Adaptive, Decentralized Search and Automated Response (RADAR). In: IEEE Symposium Series in Computational Intelligence 2011 (SSCI 2011) (2011)
12. Paz, T., Letendre, K., Burnside, W., Fricke, G., Moses, M.: How Ants Turn Information into Food. In: IEEE Symposium Series in Computational Intelligence 2011 (SSCI 2011) (2011)
13. Peters, R.: The ecological implications of body size. Cambridge University Press, Cambridge (1983)
14. Saenz, R., et al.: Dynamics of Influenza Virus Infection and Pathology. Journal of Virology 84(8), 3974–3983 (2010)
15. Warrender, C.: CyCells (Open source software) (2003), http://sourceforge.net/projects/cycells
16. Warrender, C.: Modeling intercellular interactions in the peripheral immune system. Ph.D. thesis, University of New Mexico (2004)
17. Weibel, E.R.: Scaling of structural and functional variables in the respiratory system. Annual Review of Physiology 49, 147–159 (1987)
18. West, G., Brown, J., Enquist, B.: A general model for the origin of allometric scaling laws in biology. Science 276(5309), 122–126 (1997)